Adsorption of sunset yellow FCF from aqueous solution by chitosan-modified diatomite

Y. Z. Zhang, J. Li, W. J. Li and Y. Li

ABSTRACT

Sunset yellow (SY) FCF is a hazardous azo dye pollutant found in food processing effluent. This study investigates the use of diatomaceous earth with chitosan (DE@C) as a modified adsorbent for the removal of SY from wastewater. Fourier transform infrared spectroscopy results indicate the importance of functional groups during the adsorption of SY. The obtained N_2 adsorption–desorption isotherm values accord well with IUPAC type II. Our calculations determined a surface area of 69.68 $m^2\ g^{-1}$ for DE@C and an average pore diameter of 4.85 nm. Using response surface methodology, optimized conditions of process variables for dye adsorption were achieved. For the adsorption of SY onto DE@C, this study establishes mathematical models for the optimization of pH, contact time and initial dye concentration. Contact time plays a greater role in the adsorption process than either pH or initial dye concentration. According to the adjusted correlation coefficient (adj-$R^2 > 0.97$), the models used here are suitable for illustration of the adsorption process. Theoretical experimental conditions included a pH of 2.40, initial dye concentration of 113 mg L^{-1} and 30.37 minutes of contact time. Experimental values for the adsorption rate (92.54%) were close to the values predicted by the models (95.29%).

Key words | adsorption, diatomite earth@chitosan, dye, sunset yellow

Y. Z. Zhang
J. Li (corresponding author)
W. J. Li
Y. Li
The College of Architecture and Civil Engineering,
The Key Laboratory of Beijing for Water Quality Science & Water Environment Recovery Engineering,
Beijing University of Technology,
Beijing,
100124,
China
E-mail: *lijunbjut@163.com*

INTRODUCTION

According to statistics, around 7×10^5 to 10×10^5 tons of dye are produced every year worldwide (Ghaedia *et al.* 2012). Most of the dye produced is used in textile manufacture, where total fixed dye is less than dye applied, such that more than 5–10% enters the environment through wastewater (Gupta & Suhas 2009). In some places, like NE USA, most rivers are polluted by dye, paint pigments, and/or polychlorinated biphenyls. New pollution is prevented by law, but the damage is already done. This statement would apply mostly to newly developed nations. Azo dyes and products of their decomposition introduce toxicity to aquatic environments, inducing cell mutation that can lead to cancer (Mittal *et al.* 2014). Sunset yellow (SY) is a type of pyrazolone dyestuff (anionic dye), typically used in food production, including beverages, candies, dairy and bakery products (Ghaedia *et al.* 2012).

Various physical and chemical methods have been applied to the treatment of dyes, such as chemical coagulation, flocculation and precipitation, oxidation, photocatalytic processes and membrane separation (Apostol *et al.* 2012). Most of the above technologies remove dyes effectively, but in developing countries, their initial operating cost is too high to be widely used. Adsorption is a particularly common and efficient wastewater treatment technology, favored for its convenience and efficiency (Rafatullah *et al.* 2009). The working principle of adsorption is the transfer of solute molecules onto the surface of an active solid and is superior to other dye removal technologies in terms of low cost, simple design, and convenient operation (Mittal *et al.* 2013). A number of reports have been published on removal of SY from aqueous solutions using different materials, such as mangrove bark (Seey & Kassim 2012), layered double hydroxide (LDH-MAN 4 and CaAl-LDH-NO_3) (De Sá *et al.* 2013; Malek & Yasin 2013) and layered double hydroxide (PDVB-IL) (Gao *et al.* 2013).

As a non-toxic and environmentally friendly mineral material, diatomite (diatomaceous earth), in common with vermiculite, zeolite and montmorillonite, possesses a microporous structure and large specific surface area (Sljivic *et al.* 2009). Diatomite particles contain active silicon

doi: 10.2166/wst.2015.412

hydroxyl groups, where a hydrogen ion transfers to silicon hydroxyl in the aqueous solution, negatively charging the diatomite surface (Khalighi Sheshdeh *et al.* 2012). Although cationic dyes are readily adsorbed by diatomite, anionic dyes are hardly adsorbed by natural diatomite. In addition, natural diatomite has many advantages, but adsorption performance of natural diatomite requires improvement for industrial use. Thus, natural diatomite is modified by many methods for removal of dye from effluent. For example, the removal of methylene blue aqueous solution by manganese oxide compounded with diatomite has been reported (Al-Ghouti *et al.* 2007). Physical and chemical modification methods have also been investigated. Al-Ghouti *et al.* (2009) introduced oxide–nanoparticle-modified diatomite to adsorb Basic Red 46. Zhang (Zhang *et al.* 2013) studied methylene blue adsorption on diatomite treated with sodium hydroxide. The above-mentioned methods have been studied for many years; nevertheless, there are some disadvantages to the currently introduced adsorbents, such as high water use, high cost and insufficient adsorption capacity.

Therefore, the focus of this work was to modify diatomite by chitosan to improve its adsorption capacity for SY. Herein, we introduce a new modified technology, based on chitosan's characteristic positive charge in acidic solution, to prepare diatomaceous earth with chitosan (DE@C) as a potential adsorbent of SY from water. No previous study has described the adsorption of SY by DE@C, however. In order to achieve the optimal conditions for dye adsorption, the process variables were optimized using response surface methodology (RSM). Once this optimizing process was complete, removal capacity of DE@C was evaluated by Fourier transform infrared (FT-IR) analysis, the Barrett–Joyner–Halenda (BJH) method and fluorescence spectroscopy.

MATERIALS AND METHODS

Preparation of raw diatomite

The white diatomite was supplied by Tianfu Colloidal Co., Ltd (Jilin Province, China) and was ground to about 80 mesh (Figure 1(a)).

Synthesis of the diatomite with chitosan

The diatomite was first cleaned and modified with chitosan. In this process, 100 g of diatomite was mixed at 3% ($v\,v^{-1}$) with acetic acid solution, at 25 °C for 6 hours, to remove surface impurities, then suction filtered. Next, 8 g of chitosan

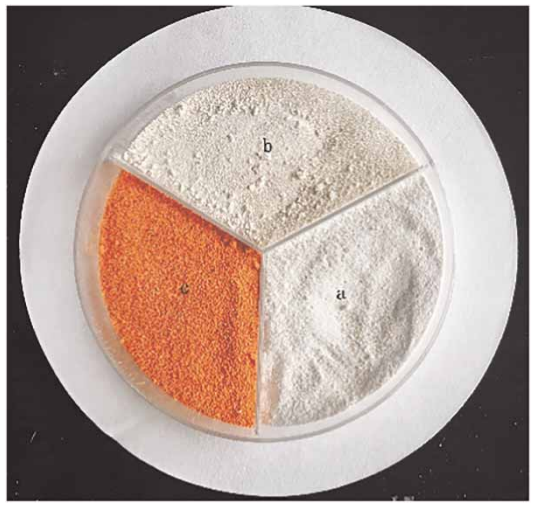

Figure 1 | (a) Image of raw diatomite. (b) Image of diatomite earth@chitosan. (c) Image of diatomite earth@chitosan after adsorption.

was added to 3% ($v\,v^{-1}$) acetic acid solution at a volume rate of 1000 mL $L^{-1}$and stirred until the chitosan completely dissolved, producing a light-yellow viscous solution. To this solution, 100 g diatomite was added using a magnetic stirrer at 500 rpm and 25 °C for 12 hours. The DE@C was obtained by suction filtration and drying at 105 °C. At last, the obtained DE@C was milled to about 80 mesh (Figure 1(b)). Between raw diatomite and prepared DE@C, the color did not change significantly. However, when the adsorption process finished, the color of DE@C changed from white to saffron (Figure 1(c)).

Reagents

Sunset yellow, molecular formula = $C_{16}H_{10}N_2Na_2O_7S_2$, molecular weight = 452.37, λ_{max} = 482 nm, is an acid dyestuff. Its pigment ions are negatively charged. Here, SY was prepared as a 1000 mg L^{-1} solution and used as the stock solution in all subsequent experiments. Chitosan (deacetylation degree of 85 ± 5%) was purchased from Sinopharm Chemical Reagent Co., Ltd. Other reagents used in the experiments were of analytic quality.

Instrumentation and analytical method

The ultraviolet–visible spectrophotometer, UV-765, was manufactured by Shanghai Precision and Scientific Instrument Co., Ltd. The FT-IR meter, Alpha infrared spectrometer, was made by Bruker, in Germany. pH was measured by a WTW meter (MTQ/TC2020, Germany). BET (Brunauer–Emmett–Teller) surface area and BJH pore

size distribution were measured by a specific surface analyzer (Micromeritics ASAP 2020, USA).

In this experiment, the absorbance of SY was measured by an ultraviolet–visible spectrophotometer at 482 nm, and the concentration of dye in solution was calculated according to the standard curve. Before and after adsorption of dye to DE@C, FT-IR spectrometry was recorded at wavelengths ranging from 4000 to 500 cm^{-1}, with a resolution of 4 cm^{-1}. The BET surface area of DE@C was measured in the relative pressure range from 0.05 to 0.4. Defined as the volume of liquid nitrogen corresponding to the adsorbed amount, the total pore volume was measured at a single point, where $P/P_0 = 0.987$. The pore size distributions were deduced from N_2 adsorption isotherms using the BJH method (Tseng & Tseng 2006). Before measurements, DE@C was analyzed by adsorption/desorption test, using liquid nitrogen at 77 K and degassing for 15 hours at 250 °C in the appropriate port of the adsorption analyzer.

Batch adsorption tests

Before adsorption, the DE@C was washed three times with distilled water to remove any soluble ions from its surface. SY solution was dosed with 2 g DE@C in an Erlenmeyer flask (capacity 1000 mg L^{-1}), and then placed in a constant magnetic stirrer (85-2A, JinTan RongHua Instruments, China), held at 20 °C and 150 rpm throughout. The experiments were performed at different initial concentration of SY (50, 100 and 150 mg L^{-1}), for various contact periods (0, 20 and 40 minutes) and at varied pH (2, 4 and 6). During batch adsorption, solution pH was regulated by 1 mol L^{-1} HCl and 1 mol L^{-1} NaOH. In order to ensure consistency of all operation steps, the liquid supernatant was assimilated, centrifuged at 3200 rpm for 2 minutes, then measured via ultraviolet spectrophotometry. Adsorption rate was determined by comparing dye concentration before and after adsorption. The removal rate of SY is computed as follows:

$$\text{Removal rate } (Y) = \frac{V(C_0 - C_e)}{C_0} \times 100 \quad (1)$$

where C_0 is the initial concentration of SY in solution (mg L^{-1}), C_e is the liquid phase dye concentration at equilibrium (mg L^{-1}) and V is the volume of the solution (L).

Experimental design

Response surface methodology is commonly used in the field of biological, chemical and pharmaceutical engineering screening and process optimization (Vučurović *et al.* 2014). The response surface method is widely used for fitting the relationship between multiple factors and response values, using multiple regression equations, and to estimate the coefficient of regression equations. In turn, these results are applied to achieve the objective of the process and optimization of parameters by calculating the extreme value or the target value. In this study, RSM was applied to optimize the adsorption experiments. Using Stat-Ease software (Design-Expert 8.0.6 Trial, Minneapolis, MN, USA), experimental design and data analysis were performed.

The effect of three experimental variables on the removal rate of SY (response value) were investigated according to Box–Behnken design (BBD) at three levels: pH (X_1), initial concentration of SY as mg L^{-1} (X_2) and contact time in minutes (X_3). The sum of 17 experiments from the study were applied toward the construction of a quadratic model. The experimental ranges and the levels of independent variables are given in Table 1. A quadratic second-degree polynomial equation approximated in this study can be expressed as:

$$Y = +\alpha_0 + \alpha_1 X_1 - \alpha_2 X_2 + \alpha_3 X_3 - \alpha_{12} X_1 X_2 - \alpha_{13} X_1 X_3 - \alpha_{23} X_2 X_3 - \alpha_{11} X_1^2 + \alpha_{22} X_2^2 - \alpha_{33} X_3^2 \quad (2)$$

where Y is the response (predicted adsorption rate). X_1, X_2 and X_3 are independent variables (pH, initial dye concentration and contact time, respectively), while α_0 is the constant coefficient, α_1, α_2 and α_3 are linear coefficients, and α_{11}, α_{22}, as well as α_{33} are the quadratic coefficients. Finally, α_{12}, α_{13} and α_{23} are interaction coefficients.

Evaluation of the fitted model

Coefficients were estimated by a mathematical model for the optimization of the process, wherein the model predicts the response and finds parameters that accord with ideal experimental conditions. Choosing the level of the independent

Table 1 | Values of factors in their experimental design

		Ranges and levels		
Factor	**Name**	**−1**	**0**	**+1**
X_1	pH	2	4	6
X_2	Initial SY concentration (mg L^{-1})	100	200	300
X_3	Contact time (min)	0	20	40

Table 2 | The Box–Behnken matrix and the value of the responses

Run	X_1	X_2 (mg L^{-1})	X_3 (min)	Y_{Exp} (%)	Y_{pred} (%)
1	4.00	200.00	20.00	65.93	66.59
2	2.00	300.00	20.00	68.45	71.02
3	4.00	200.00	20.00	66.27	66.59
4	4.00	200.00	20.00	67.76	66.59
5	6.00	200.00	0.00	0.00	−0.80
6	6.00	100.00	20.00	87.61	85.04
7	4.00	100.00	40.00	89.92	95.29
8	4.00	300.00	40.00	61.31	57.94
9	6.00	300.00	20.00	48.12	54.29
10	4.00	200.00	20.00	66.32	66.59
11	6.00	200.00	40.00	74.18	71.38
12	2.00	100.00	20.00	92.54	86.37
13	4.00	200.00	20.00	66.64	66.59
14	4.00	100.00	0.00	0.00	3.37
15	4.00	300.00	0.00	0.00	−1.37
16	2.00	200.00	40.00	85.06	85.85
17	2.00	200.00	0.00	0.00	2.80

variables primarily affects the extent of adsorption by DE@C; the parameters are given in Table 2. The suitability of the fitted, second-order polynomial models were evaluated by some important methods, and the results were assessed using analysis of variance (ANOVA) (R^2, adj-R^2, F-value at a probability P of 0.05).

RESULTS AND DISCUSSION

Characteristics of the adsorbent

FT-IR analysis

DE@C possesses significantly greater adsorption capacity than untreated diatomite. In order to investigate why, we explored the surface functional groups of diatomite by FT-IR analysis in the range of 500–4000 cm^{-1}. Figure 2 shows the FT-IR spectra for chitosan, raw diatomite, DE@C and DE@C after adsorption. In Figure 2(b), the main spectral peaks of functional groups are detected at

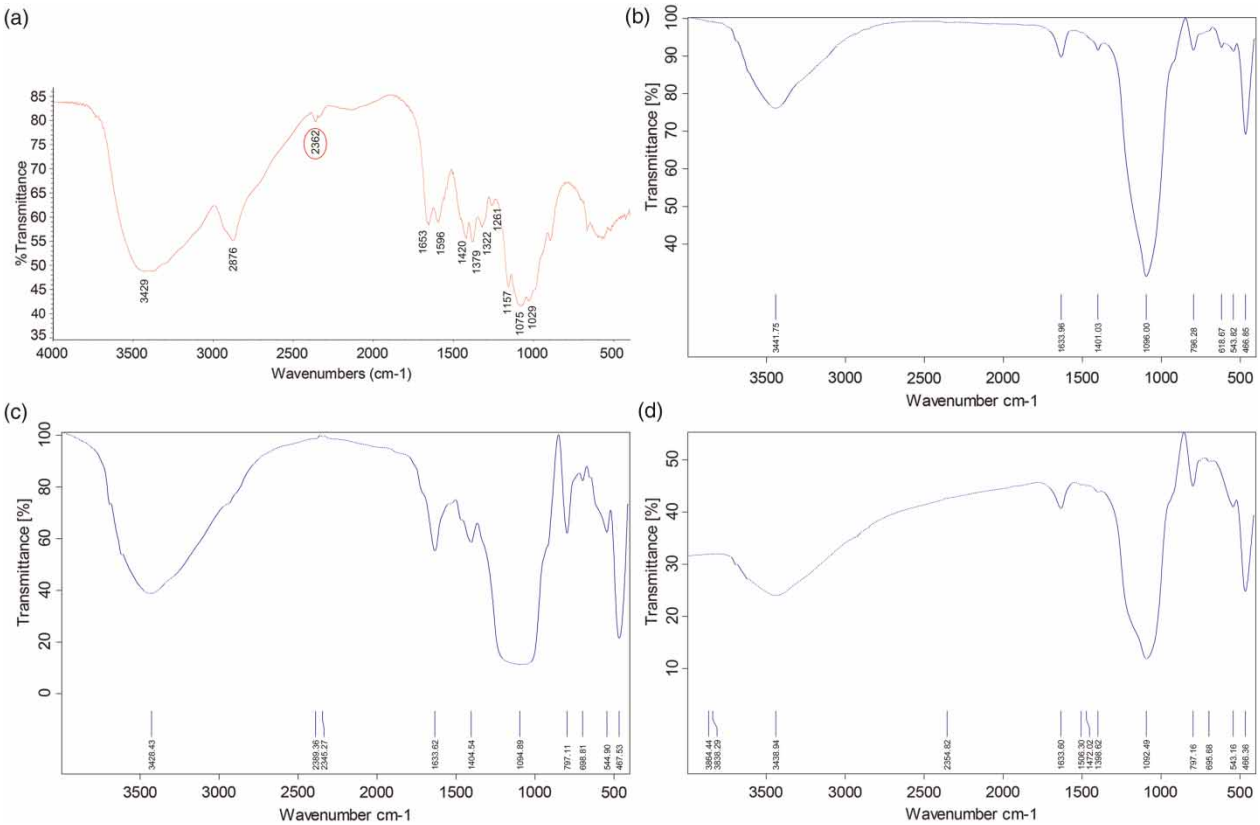

Figure 2 | (a) FT-IR spectra of chitosan. FT-IR spectra of adsorbents: (b) raw diatomite, (c) DE@C and (d) DE@C after adsorption.

3429, 2876, 2362, 1653, 1596, 1420, 1379, 1322, 1261, 1157, 1075 and 1029. The peak at 2362 cm^{-1} may be caused by the amino group (–NH_2) and amino group (–NH_2) plays an important role for adsorption of SY.

According to Equations (3)–(5), as an anionic dye, SY will produce anionic ion (SO_3^-) in aqueous solutions. The ionic interactions of the colored dye ions (D–SO_3Na) with the amino groups (R–NH_2) on the DE@C may be the possible mechanisms of SY adsorption. In the presence of H^+, the amino groups of modified diatomite (DE@C–NH_2) were protonated.

$$D - SO_3Na \xrightarrow{H_2O} D - SO_3^- + Na^+ \quad (3)$$

In aqueous solution, SY is dissolved and then the sulfonate groups is dissociated and converted to anionic dye ions.

$$DE@C - NH_2 + H^+ \rightleftharpoons DE@C - NH_3^+ \quad (4)$$

The adsorption process then proceeds because of the electrostatic attraction between these two counter ions.

$$DE@C - NH_3^+ + D - SO_3^- \rightleftharpoons DE@C - NH_3^+O_3S - D \quad (5)$$

Compared with DE@C, there is no amino group peak in raw diatomite (Figure 2(b)). After modification, at 2389 and 2346 cm^{-1}, which are caused by the amino group appeared in DE@C (Figure 2(c)). This phenomenon demonstrated SY can be adsorbed effectively after the modification.

In Figure 2(b), the main spectral peaks of functional groups are detected at 3442, 1634, 1401, 1096, 796 and 618 cm^{-1}. The peak at 3442 cm^{-1} may be attributed to the hydrogen atom attached to Si–H. The peak at 1634 cm^{-1} is likely caused by flexural vibration of H–OH. The peak at 1401 cm^{-1} is due to stretching vibration of C–O and flexural vibration of H–OH. The peak at 1096 cm^{-1} is attributed to Si–O–H. The peaks at 796 and 618 cm^{-1} are the result of flexural vibration by Si–O–Si or Si–O.

Major key peaks in the spectra of raw diatomite and DE@C are similar. When compared to raw diatomite, two new peaks appear in the spectra of DE@C (Figure 2(c)), at 2389 and 2346 cm^{-1}, which are caused by the amino group (–NH_2). The spectra of DE@C after adsorption (Figure 2(d)) shows three new peaks compared to raw diatomite. These peaks at 2354 cm^{-1} are also caused by the amino group (–NH_2). The peak at 1506 cm^{-1} may be caused by the stretching vibration of C=C, while the peak at 1398 cm^{-1} may be attributed to C–O. What is more, an organic peak is found at 1472 cm^{-1} (–CH_2). According to the amino group (–NH_2) peak, we speculate that diatomite is successfully modified with chitosan (Wong *et al.* 2003). As well, the increases in characteristic peaks may be evidence for efficient adsorption by modified DE@C.

BET analysis

Figure 3(a) shows the N_2 adsorption–desorption isotherm values for DE@C. The obtained N_2 adsorption isotherm values accord well with type II isotherm (in IUPAC classification) (Rouquerol *et al.* 1994), which refers to a multi-layer reversible adsorption process, in this case, interaction between DE@C and SY. There is a clear H4-type hysteresis loop from $P/P_0 = 0.40$ to 0.98. The attribute of H4-type hysteresis loop, which does not exhibit any limiting adsorption at high P/P_0, is observed when aggregates of slit-like particles give rise to narrow slit-shaped pores (Sing 1985).

Figure 3(b) shows distribution of DE@C pore size on the basis of the BJH model. Using the BET equation (Sing 1985), we obtained a calculated surface area for DE@C of 69.68 $m^2\,g^{-1}$. Respective total pore volume and average pore diameters were 0.1209 $cm^3\,g^{-1}$ and 4.85 nm. There are many kinds of diatomite in the world, and many factors affect the surface area. Although DE@C possesses decreased surface area compared to raw diatomite, the determined

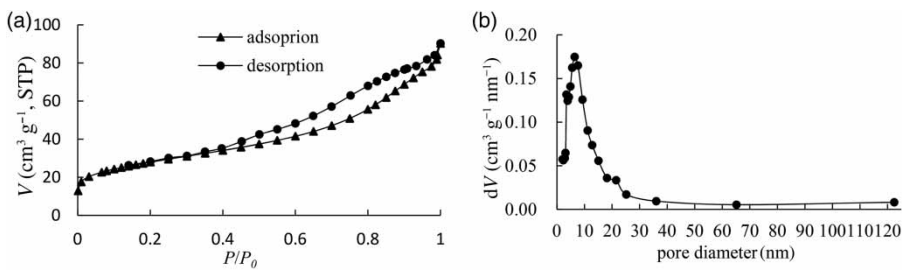

Figure 3 | (a) N_2 adsorption/desorption isotherm of DE@C and (b) BJH pore size distribution. (STP: standard temperature and pressure).

surface area value was greater than that of calcined diatomite ($52.56\ m^2\ g^{-1}$), as reported by Lin *et al.* (2007). Therefore, BET surface area and total pore volume of DE@C suggest it is a superior porous adsorbent.

Response surface model analysis and optimization

Important factors that have great influence on the adsorption process of a modified adsorbent, such as DE@C, are pH, initial concentration and contact time. In order to evaluate optimal conditions and study the influence of factors on SY adsorption, our experiments were investigated according to BBD design. By multiple regression analysis, the removal rate (Y) of SY was predicted in accordance with Equation (2) and Table 2. Referring to response surface 3D plots (Figure 4), regression coefficients were generated to explain the influence of three process parameters on the adsorption rate. The relevance of the fitting model was evaluated by correlation coefficient (Adj-R^2). Applying ANOVA, the adequacy and statistical significance of the quadratic models were evaluated, and the results are summarized in Table 3. The regression models were significant at a 95% confidence level. The fitting-degree coefficient values are more suitable for evaluation models ($R^2 > 0.98$). This result implies that the fitting degree is good, and that at least 98% of the variations which occurred in the response are predicted by the model equations.

According to the removal of SY by DE@C, we observed (Table 3) that the quadratic model (Y) demonstrated significance and sufficiency (F-value = 73.39 and $P < 0.0001$), with only 2.4% of total variation not illustrated by the model (Adj-$R^2 = 0.9760$). Figure 4 depicts the response surface 3D plots of the individual and interactive effects of process parameters on the rate of DE@C for adsorption of SY. The 3D plots were used to adjust two variables within experimental range, while the third variable remains unchanged. Figure 4(a) shows that higher adsorption rate was obtained at lower values of pH and initial dye concentration. It can be seen that adsorption equilibrium was achieved and adsorption rate reached the highest at about 32 minutes (Figure 4(b)). Figure 4(c) also shows that adsorption rate is higher at lower initial dye concentration. The model terms X_1, X_2, X_3, X_2X_3 and ${X_3}^2$ are significant ($P < 0.05$) while X_1X_2, X_1X_3, ${X_1}^2$ and ${X_2}^2$ do not have a significant effect on adsorption rate (Table 3). A positive coefficient sign indicates a mutual effect, but a negative sign indicates an opposite effect on response (Roy *et al.* 2012). On one hand, adsorption rate was impacted by X_3, ${X_1}^2$ and quadratic terms of ${X_2}^2$. On the other hand, X_1, X_2, plus reciprocities between X_1 and X_3, X_1 and X_2, X_2 and X_3, and ${X_3}^2$ have a negative effect on adsorption rate.

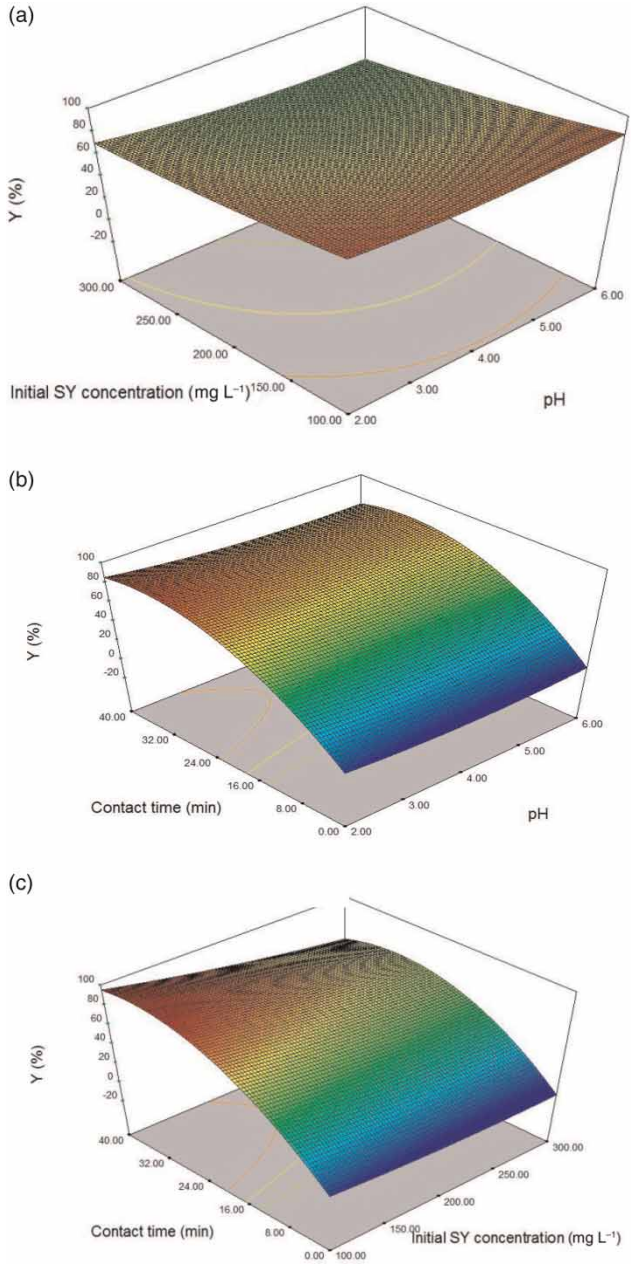

Figure 4 | Response surface plots (3D) showing the effects of (a) pH and initial dye concentration, (b) pH and contact time, (c) contact time and initial dye concentration, and their influence on adsorption rate for removal of SY.

Furthermore, in order to verify the accuracy between experimental values and predicted values, optimization of investigated variables for SY removal with DE@C was carried out. Through Design Expert software, we calculated the maximal adsorption rate for removal of SY at 95.29%. When the corresponding optimal theoretical experimental

Table 3 | Analysis of variance (ANOVA) for the experimental results

Source	*F*-value *Y*	*P*-value *Y*
Model	73.39	<0.0001*
X_1	6.05	0.0434*
X_2	39.40	0.0004*
X_3	446.70	<0.0001*
X_1X_2	2.20	0.1816**
X_1X_3	1.10	0.3299**
X_2X_3	7.59	0.0283*
X_1^2	3.59	0.0998**
X_2^2	1.22	0.3057**
X_3^2	155.64	<0.0001*

*Significant at $P < 0.05$.
**Not significant.
SY: $R^2 = 0.9895$, Adjusted $R^2 = 0.9760$.

conditions were pH 2.40, an initial dye concentration of 113 mg L^{-1} and 30.37 minutes of contact time, the predicted optimal values for SY removal by DE@C proved to be accurate. The models were consistently accurate over repeated experiments (three replicates). The real optimal adsorption rate was determined to be 92.54%, which is very close to the theoretical value.

$$Y = +66.59 - 4.52X_1 - 11.52X_2 + 38.81X_3 - 3.85X_1X_2 - 2.72X_1X_3 - 7.15X_2X_3 + 4.80X_1^2 + 2.80X_2^2 - 31.58X_3^2 \quad (6)$$

CONCLUSION

This novel investigation demonstrates that DE@C, a low-cost adsorbent, exhibits excellent adsorption capacity for SY. FT-IR results indicate that functional groups play an important role during the adsorption of SY. Our observations indicate that efficient adsorption capacity is due to the presence of multiple functional groups on the DE@C surface. The BET and BJH results showed that DE@C also had a larger specific surface area (69.68 $m^2 g^{-1}$) than that of calcined diatomite (52.56 $m^2 g^{-1}$), as reported by Lin *et al.* (2007). Regarding the adsorption of SY onto DE@C, this work introduces the mathematical models for the optimization of pH (2–6), contact time (0–40 minutes) and initial dye concentration (100–300 mg L^{-1}). Through RSM analysis, contact time was shown to have an important influence on adsorption of SY onto DE@C. On the basis of adjusted correlation coefficient, the models used demonstrate suitability for illustration of the adsorption process. Experimental values for adsorption rate ($Y > 95\%$) were close to those values predicted by the models. Overall, we find in diatomaceous earth compounded with chitosan a potential low-cost, efficient adsorbent for the removal of sunset yellow FCF.

ACKNOWLEDGEMENT

The work was supported by the Building water system microcirculation reconstruction technology research and demonstration project (2014ZX07406002).

REFERENCES

Al-Ghouti, M. A., Khraisheh, M. A. M., Ahmad, M. N. & Allen, S. J. 2007 Microcolumn studies of dye adsorption onto manganese oxides modified diatomite. *Journal of Hazardous Materials* **146** (1–2), 316–327.

Al-Ghouti, M. A., Al-Degs, Y. S., Khraisheh, M. A. M., Ahmad, M. N. & Allen, S. J. 2009 Mechanisms and chemistry of dye adsorption on manganese oxides-modified diatomite. *Journal of Environmental Management* **90** (11), 3520–3527.

Apostol, L. C., Pereira, L., Pereira, R., Gavrilescu, M. & Alves, M. M. 2012 Biological decolorization of xanthene dyes by anaerobic granular biomass. *Biodegradation* **23**, 725–737.

De Sá, F. P., Cunha, B. N. & Nunes, L. M. 2013 Effect of pH on the adsorption of sunset yellow FCF food dye into a layered double hydroxide (CaAl-LDH-NO_3). *Chemical Engineering Journal* **215**, 122–127.

Gao, H. J., Kan, T. T., Zhao, S. Y., Qian, Y. X., Cheng, X. Y., Wu, W. L., Wang, X. D. & Zheng, L. Q. 2013 Removal of anionic azo dyes from aqueous solution by functional ionic liquid cross-linked polymer. *Journal of Hazardous Materials* **261**, 83–90.

Ghaedia, M., Hekmati Jah, A., Khodadoust, S., Sahraei, R., Daneshfar, A., Mihandoost, A. & Purkait, M. K. 2012 Cadmium telluride nanoparticles loaded on activated carbon as adsorbent for removal of sunset yellow. *Spectrochimica Acta Part A: Molecular and Biomolecular Spectroscopy* **90**, 22–27.

Gupta, V. K. & Suhas 2009 Application of low-cost adsorbents for dye removal. *Journal of Environmental Management* **90**, 2313–2342.

Khalighi Sheshdeh, R., Khosravi Nikou, M. R., Badii, Kh. & Yousefi Limaee, N. 2012 Adsorption of basic organic colorants from an aqua binary mixture by diatomite. *Progress in Color, Colorants and Coatings* **5**, 101–116.

Lin, J. X., Zhan, S. L., Fang, M. H. & Qian, X. Q. 2007 The adsorption of dyes from aqueous solution using diatomite. *Journal of Porous Materials* **14** (4), 449–455.

Malek, A. H. A. & Yasin, Y. 2012 Use of layered double hydroxides to remove sunset yellow FCF dye from aqueous solution. *Chemical Science Transactions* **1**, 194–200.

Mittal, J., Thakur, V. & Mittal, A. 2013 Batch removal of hazardous azo dye Bismark Brown R using waste material hen feather. *Ecological Engineering* **60**, 249–253.

Mittal, A., Thakura, V., Mittala, J. & Vardhan, H. 2014 Process development for the removal of hazardous anionic azo dye Congo red from wastewater by using hen feather as potential adsorbent. *Desalination and Water Treatment* **52**, 227–237.

Rafatullah, M., Sulaiman, O., Hashim, R. & Ahmad, A. 2009 Adsorption of copper (II), chromium (III), nickel (II) and lead (II) ions from aqueous solutions by Meranti sawdust. *Journal of Hazardous Materials* **170**, 969–977.

Rouquerol, J., Avnir, D., Fairbridge, C. W., Everett, D. H., Haynes, J. M., Pernicone, N. & Unger, K. K. 1994 Recommendations for the characterization of porous solids. *Pure and Applied Chemistry* **66** (8), 1739–1758.

Roy, A., Chakraborty, S., Kundu, S. P., Adhikari, B. & Majmunder, S. B. 2012 Adsorption of anionic-azo dye from aqueous solution by lignocellulose-biomass jute fiber: equilibrium, kinetics, and thermodynamics study. *Industrial & Engineering Chemistry Research* **51**, 12095–12106.

Seey, T. L. & Kassim, M. J. N. M. 2012 Acidic and basic dyes removal by adsorption on chemically treated mangrove barks. *International Journal of Applied Science and Technology* **2**, 270–276.

Sing, K. S. W. 1985 Reporting physisorption data for gas/solid systems with special reference to the determination of surface area and porosity (Recommendations 1984). *Pure and Applied Chemistry* **57** (4), 603–619.

Sljivic, M., Smičiklas, I., Pejanović, S. & Plećaš, I. 2009 Comparative study of Cu^{2+} adsorption on a zeolite, a clay and a diatomite from Serbia. *Applied Clay Science* **43** (1), 33–40.

Tseng, R. L. & Tseng, S. K. 2006 Characterization and use of high surface area activated carbons prepared from cane pith for liquid-phase adsorption. *Journal of Hazardous Materials* **136** (3), 671–680.

Vučurović, V. M., Razmovski, R. N., Miljić, U. D. & Puškaš, V. S. 2014 Removal of cationic and anionic azo dyes from aqueous solutions by adsorption on maize stem tissue. *Journal of the Taiwan Institute of Chemical Engineers* **45** (4), 1700–1708.

Wong, Y. C., Szeto, Y. S., Cheung, W. H. & Mckay, G. 2003 Equilibrium studies for acid dye adsorption onto chitosan. *Langmuir* **219** (19), 7888–7894.

Zhang, J., Ping, Q. W., Niu, M. H., Shi, H. Q. & Li, N. 2013 Kinetics and equilibrium studies from the methylene blue adsorption on diatomite treated with sodium hydroxide. *Applied Clay Science* **83–84**, 12–16.

First received 9 April 2015; accepted in revised form 22 July 2015. Available online 4 August 2015